Dalton Transactions

Accepted Manuscript

This article can be cited before page numbers have been issued, to do this please use: D. Strohecker, V. Lynch, B. Holliday and R. A. Jones, *Dalton Trans.*, 2017, DOI: 10.1039/C7DT01153A.

ROYAL SOCIETY OF CHEMISTRY

rsc.li/dalton

View Article Online
DOI: 10.1039/C7DT01153A

Chemical Science

ARTICLE

Synthesis and Electronic Investigation of Mono- and Di-substituted 4-Nitro- and 4-Amino-pyrazol-1-yl Bis(pyrazol-1-yl)pyridine-type Ligands and Luminescent Eu(III) Derivatives

Received 00th January 20xx,
Accepted 00th January 20xx

DOI: 10.1039/x0xx00000x

www.rsc.org/

D. J. Strohecker,[a] V. M. Lynch,[a] B. J. Holliday† and R. A. Jones[a]†

Four new disubstituted and monosubstituted nitro- and amino- bis(pyrazol-1-yl)pyridine (bppy) ligands, substituted at the pyrazole 4-position (**1**, **2**, **5**, **6**) have been synthesized, along with two luminescent Eu(III) tris-β-diketonate derivatives of the amino substituted ligands (**7**, **8**). The compounds have been studied using UV-Vis absorbance spectroscopy and cyclic voltammetry which has allowed for characterization of the electronic environments of these ligands. The calculated HOMO-LUMO gap values (**1**: 3.54 eV; **2**: 3.53 eV; **5**: 3.01 eV; **6**: 3.66 eV) differ from that of bppy (3.86 eV) and the range is indicative that tuning of the ligand electronic environment is possible. Additionally, fluorescence spectroscopy studies were employed to determine ligand T_1 energy levels of the amine-bearing ligands **2** and **6**, yielding values of T_1 of 25,381 cm^{-1} and 26,201 cm^{-1}, respectively. These ligands were employed in the synthesis of Eu(III) complexes **7** and **8**, for which the absolute and intrinsic quantum yields, lifetimes and ligand sensitization efficiencies were determined.

Introduction

Lanthanide complexes continue to be of significant interest for potential applications in magnetism, optoelectronics and as probes in biological systems.[1–4] The useful photophysical properties of certain lanthanide complexes include large pseudo-Stokes shifts, discreet emission wavelengths and long lifetimes. Due to their ease of synthesis and favourable emissive properties lanthanide complexes of multidentate ligands containing pyridyl or pyrazolyl groups, or both, are now well established. Two of the most important ligands of this class are, 2,6-bis(pyrazol-1-yl)pyridine (bppy) and 2,6-bis(2-pyridyl)pyridine (terpy) (Figure 1). First reported in the pioneering work by Jameson et al. in 1989, bppy has been shown to serve as a versatile analogue to the well-known tridentate nitrogen-donor terpy.[5] With respect to terpy, bppy is a weaker σ-donor as well as a weaker π-acceptor, owing to the lesser basicity of pyrazole in addition to a higher π* energy of the aromatic system, resulting in lessened ligand binding strength.[5] This deviation in electronic behavior in a ligand that is otherwise structurally similar to terpy, along with the synthetic ease with which bppy may be derivatized on the 4-position of pyridine, as well as the 3- and 5-positions of the pyrazole rings, has led to the increasing popularity of bppy as a complementary platform for research into new d- and f-block metal complexes. Halcrow published an especially thorough review of such ligands and complexes as they pertain to catalysis, dye-sensitized solar cells, spin-crossover materials, and emissive materials for LEDs and biomarkers, with a special interest taken on spin-crossover and luminescent lanthanide complexes.[6]

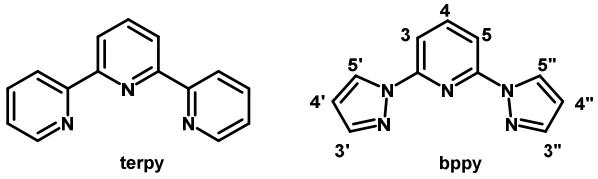

Figure 1: depiction of tridentate N-donor ligands terpy and bppy.

As Zoppellaro and Baumgarten reported in 2005, bppy derivatives substituted on the 4-position of the pyrazole ring are relatively rare, due to unwieldy synthetic routes involving non-selective lithiations or protection/deprotection steps.[7] There are consequently few examples of this type of substitution, being limited to a handful of (4-halopyrazol-1-yl)pyridines, a modest number of carbon-coupling reaction products of these compounds, and some carbonyl-derived ligands, either stemming from the formylation of said (4-halopyrazol-1-yl)pyridines or nucleophilic substitution of 2,6-dibromopyridine with ethyl pyrazole-4-carboxylate.[7–15]

Numerous heteroleptic lanthanide complexes consisting of mixed hard O- and N-chelating ligands have been reported which exhibit promising photoluminescent properties and stability; as such these motifs are desireable targets for luminescent materials.[16–21] Herein, we report the synthesis and electronic properties of the 4,4" symmetrically substituted di-nitro and di-amino derivatives $(NO_2)_2$bppy (**1**), $(NH_2)_2$bppy)

[a] *Department of Chemistry, The University of Texas at Austin, 105 E. 24th Street, Stop A5300, Austin, Texas 78712-1224, United States.*
† Corresponding author email: R. A. Jones – rajones@cm.utexas.edu; B. J. Holliday – hollidaybj@hotmail.com.
Electronic Supplementary Information (ESI) available: [details of any supplementary information available should be included here]. See DOI: 10.1039/x0xx00000x

View Article Online
DOI: 10.1039/C7DT01153A

(**2**), the 4-mono-substituted NO_2bppy (**5**) and NH_2bppy (**6**) compounds as well as the synthesis and spectroscopic characterization of two Eu(III) derivatives of the amino substituted ligands, $Eu(tta)_3(NH_2)_2$bppy (**7**) and $Eu(tta)_3NH_2$bppy (**8**) (tta = 2-thenoylacetonate) (Scheme 1).

Experimental

Materials and Methods

All reagents were purchased from commercial sources and used without further purification. Dry diglyme was obtained from Sigma-Aldrich in Sure/Seal™ bottles and used without further drying. $Eu(tta)_3 \bullet 2H_2O$ was synthesized via a literature procedure and the crystalline product was characterized by LRMS and melting-point determination.[22] Dry acetonitrile (MeCN) for electrochemical measurements was obtained using an Innovative Technology PureSolv 400 solvent purifier with a double purifying column and stored in Schlenk storage flasks over 3 Å molecular sieves under nitrogen atmosphere.

Single-crystals for X-ray diffraction studies on **3** (see ESI), **5**

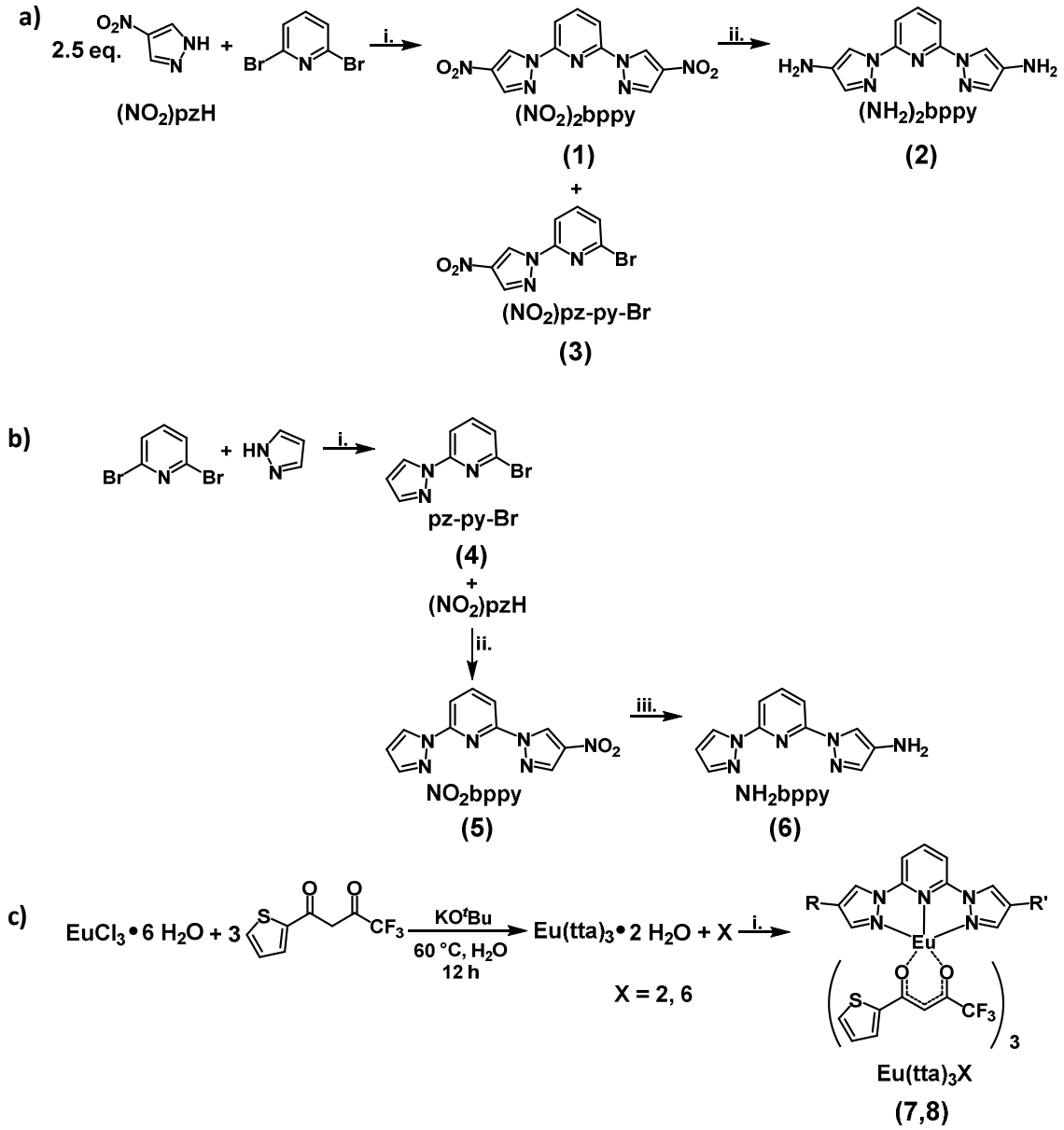

Scheme 1: **a)** Synthesis of **1** and **2**. i. NaH, N_2, 120 °C, 7 d; yield = 93% ii. 20% PtO_2, 2:3 EtOH: ethyl acetate, H_2 3 d; yield = 81% **b)** Synthesis of **5** and **6**. i. NaH, N_2, 70 °C, 2 d; yield = 50% ii. NaH, N_2, 120 °C 4 d; yield = 89% iii. 10% PtO_2, 1:1 EtOH: ethyl acetate, 25 – 45°C H_2 2 d; yield = 70% **c)** Synthesis of **7** and **8**. i. refluxing acetone, 1 d; **7**: R = R'= NH_2, yield = 76%; **8**: R = H, R' = NH_2, yield = 46%.

View Article Online
DOI: 10.1039/C7DT01153A

and **6** were grown by slow evaporation of saturated dichloromethane solutions (see supplemental information (SI)). Diffraction data for **5** were collected on a Rigaku AFC12 diffractometer with a Saturn 724+ CCD using a graphite monochromator with MoKα radiation (λ = 0.71073Å) at 100 K with the use of a Rigaku XStream low temperature device. Diffraction data for **3** and **6** data were collected on an Agilent Technologies SuperNova Dual Source diffractometer using a μ-focus Cu Kα radiation source (λ = 1.5418Å) with collimating mirror monochromators at 100 K (**3**) and 173 K (**6**) with the use of an Oxford Cryostream low temperature device. X-ray powder diffraction data of **3** was obtained on the same Agilent Technologies instrument, but powder diffraction data of **5** and **6** were collected on a Rigaku R-Axis Spider diffractometer with an image plate detector utilizing a graphite monochrometer, CuKα radiation (λ = 1.5418 Å) and Rigaku RINT RAPID control software for system automation. Further information regarding crystal structure data including powder diffraction data, refinement details, and tables of select bond lengths and angles is provided in the SI.

UV-Vis absorption spectrophotometry and fluorescence spectroscopy excitation/emission measurements were performed in Starna quartz fluorometer cells with 1.0 cm path lengths. All room-temperature solution absorption, excitation and emission spectra were obtained in dichloromethane (DCM) solvent. Luminescence measurements were recorded on a Photon Technology International QuantaMaster 4 spectrofluorometer equipped with a calibrated 6-in. diameter K Sphere-B integrating sphere used for absolute quantum yield (Φ^{L}_{Eu}) measurements. All excitation spectra were obtained by monitoring the maximum emission wavelength of the molecule; all emission spectra were obtained by irradiation of the sample with the maximum wavelength observed in the corresponding excitation spectra. Absolute quantum yields were calculated by dividing the area under the emission peak of the complex by the difference between the area under the excitation peak of the sample and that of either a solvent blank or solid $BaSO_4$ sample.

Electrochemical experiments were carried out in a dry box under a nitrogen atmosphere using a GPES system from Eco. Chemie B. V. in 0.1 M solutions of tetrabutylammonium hexafluorophosphate in dry MeCN at a scan rate of 0.100 V·s^{-1}. The electrochemical cell consisted of a 1.6 mm-diameter Pt button working electrode, Pt wire counter electrode and Ag/$AgNO_3$ reference electrode. All potentials were externally referenced to the ferrocene/ferrocenium (Fc/Fc^+) redox couple.

Synthesis

2,6-*bis*(4-nitropyrazol-1-yl)pyridine (1): In a dry box, 4-nitropyrazole (1.798 g, 15.90 mmol) was dissolved in dry diglyme (15 mL). To this solution NaH (0.520 g, 21.67 mmol) was added in small portions and stirred until H_2 (g) evolution ceased. 2,6-dibromopyridine (1.502 g, 6.34 mmol) was then added in one portion with stirring, and additional dry diglyme (50 mL) was added to the mixture. The resulting solution was removed from the dry box and heated in a 120 °C oil bath for 7 d under an N_2 atmosphere using standard Schlenk techniques. After cooling to room temperature, the reaction was quenched with H_2O (10 mL) and solvent was removed under vacuum to give a light brown solid. The solid was washed with deionized ice water (three x 50 mL portions), vacuum-filtered and then subjected to silica column chromatography using dichloromethane eluent. The product (R_f = 0.45) was isolated as a lustrous white needle-like crystalline solid (yield: 1.768g, 93%). ^{1}H-NMR (500 MHz, *d*-DMSO, 130 °C): 9.99 (s, 2H), 8.506 (s, 2H), 8.316 (t, 1H *J* = 1.5) 8.058 (d, 2H *J* = 6.0). $^{13}C\{^1H\}$-NMR (100 MHz, *d*-DMSO, 130 °C): 148.0, 142.8, 137.1, 137.0, 127.6, 111.6. HR-MS (CI^+): calcd for $C_{11}H_7N_7O_4$ *m/z* 301.0560, found 301.0557. IR ($\bar{\nu}$, cm^{-1}): 3,162 (s, C – H), 3,148 (m, C – H), 1,615 (m, N – O), 1,405 (s, N – O). M.P.: 344.16 – 346.10 °C. Elemental Analysis: calcd C 43.86% H 2.34% N 32.55%, found C 43.73% H 2.28% N 32.32%.

2-bromo-6-(4-pyrazol-1-yl)pyridine (3) was formed as a yellow crystalline solid by-product in yields up to 31%, in the previous reaction and isolated as the R_f = 0.8 band with silica column chromatography using dichloromethane eluent. ^{1}H NMR (400 MHz, $CDCl_3$): 9.24 (s,1H), 8.25 (s, 1H), 7.98 (d, 1H *J* = 8.0), 7.73 (t, 1H *J* = 7.9), 7.52 (d, 1H *J* = 7.8). $^{13}C\{^1H\}$-NMR (100 MHz, $CDCl_3$): 149.8, 141.3, 140.6, 137.74, 137.65, 127.8, 126.4, 111.6. HR-MS (ESI^+): calcd for $C_8H_6BrN_4O_2$ $(M + H)^+$ *m/z* 270.96490, found 270.96520. IR ($\bar{\nu}$, cm^{-1}): 2,921 (m, C – H), 1,566 (m, N – O), 1,501 (m, N – O), 1,038 m, C – Br). M.P. 136.1 – 137.5 °C. Elemental Analysis: calcd C 35.71% H 1.87% N 20.82%, found C 34.89% H 1.73% N 20.13%.

2,6-*bis*(4-aminopyrazol-1-yl)pyridine (2): $PtO_2 \bullet H_2O$ (0.0811 g, 20% catalyst loading) was suspended in a 2:3 mixture of EtOH: ethyl acetate (EtOAc) (500 mL). H_2 gas was sparged through this mixture for 1 h. **1** (0.497 g, 1.65 mmol) was then added to this mixture in one portion and the stirred suspension was sparged with H_2 gas for an additional hour then sealed under a H_2 atmosphere. The sealed reaction mixture was stirred an additional 3 d at room temperature with 1 h H_2 sparge cycles every 24 h. The reaction was then vacuum-filtered through Celite and concentrated under vacuum to yield a brown solid. The solid was subjected to silica column chromatography using a 5% v: v methanol: dichloromethane eluent. The last band (R_f = 0.15) was isolated and concentrated to give a yellow solid (yield: 0.320 g, 81%). ^{1}H-NMR (400 MHz, *d*-DMSO): 7.93 (d, 2H J = 1.0), 7.92 (t, 1H *J* = 8.0), 7.54 (d, 2H *J* = 8.0), 7.38 (d, 2H *J* = 0.98), 4.41 (s, 4H). $^{13}C\{^1H\}$-NMR (100 MHz, *d*-DMSO): 150.1, 141.5, 135.1, 134.1, 111.09, 106.54. HR-MS (CI^+): calcd for $C_{11}H_{11}N_7$ *m/z* 241.1076, found 241.1075. IR ($\bar{\nu}$, cm^{-1}): 3,310 (b, N – H), 2,962 (m, C – H), 1,603 (s, N – H), 1,577 (s, N – H), 1,259 (s, C – N amine). M.P. 168.19 – 213.16 °C (decomp.). Elemental Analysis: calcd C 54.76% H 4.60% N 40.64%, found C 54.93% H 4.41% N 38.24%. N analyses were consistently slightly low on this compound. At present we do not have a simple explanation for this.

2-bromo-6-(pyrazole-1-yl)pyridine (4): This compound was prepared following a slightly-modified literature procedure.[17] In a dry box, 1-H-pyrazole (0.657 g, 9.75 mmol) was dissolved in dry diglyme (15 mL). To this solution NaH (60 % in oil, 0.458 g, 11.41 mmol) was added in small portions and stirred until H_2

View Article Online
DOI: 10.1039/C7DT01153A

(g) evolution ceased. 2,6-dibromopyridine (2.457 g, 10.37 mmol) was then added in one portion with stirring, and additional dry diglyme (20 mL) was added to the mixture. The resulting solution was removed from the dry box and heated in a 70 °C oil bath for 2 d under an N_2 atmosphere using standard Schlenk techniques. After cooling to room temperature, the reaction was quenched with H_2O and solvent was removed to give a light brown solid. The solid was extracted with DCM, washed with H_2O then subjected to silica column chromatography using DCM eluent. The product (R_f = 0.65) was isolated as a white crystalline solid (1.17 g, 50% yield). ^{1}H-NMR (400 MHz, $CDCl_3$): 8.31 (d, 1H *J* = 2.6), 7.93 (d, 1H *J* = 8.0), 7.73 (d, 1H, *J* = 1.68), 7.65 (td, 1H *J* = 7.8, 1.2), 7.35 (d, 1H *J* = 7.72, 0.8), 6.46 (m, 1H).

2-(4-nitropyrazol-1-yl)-6-(pyrazol-1-yl)pyridine (5): In a dry box, 4-nitropyrazole (0.505 g, 4.46 mmol) was dissolved in dry diglyme (15 mL). To this solution NaH (60% wt. in oil, 0.156 g, 3.90 mmol) was added in small portions and stirred until H_2 (g) evolution ceased. **4** (0.500 g, 2.23 mmol) was then added in one portion with stirring, and additional dry diglyme (5 mL) was added to the mixture. The resulting solution was removed from the dry box and heated in a 120 °C oil bath for 4 d under an N_2 atmosphere using standard Schlenk techniques. After cooling to room temperature, the reaction was quenched with H_2O (10 mL) and solvent was removed under vacuum to give a canary-yellow solid. This solid was dissolved in DCM, washed with H_2O then subjected to silica column chromatography using DCM eluent. The product (R_f = 0.5) was isolated as a white crystalline solid (0.509 g, 89% yield). ^{1}H-NMR (400 MHz, $CDCl_3$): 9.25 (d, 1H *J* = 0.72), 8.58 (dd, 1H *J* = 2.6, 0.7), 8.29 (d, 1H *J* = 0.5), 8.07 – 7.99 (m, 2H), 7.94 – 7.87 (m, 1H), 7.82 – 7.77 (m, 1H), 6.55 (dd, 1H J = 2.6, 1.7). ^{13}C{^{1}H}-NMR (100 MHz, $CDCl_3$): 151.6, 143.1, 142.7, 137.6, 127.3, 125.9, 112.0, 110.0, 108.8. HR-MS (ESI^+): calcd for $C_{11}H_8N_6O_2$ ($[M+Na]^+$) *m/z* 279.0610, found 279.03090. IR ($\bar{\nu}$, cm^{-1}): 3,175 (s, C – H), 3,130 (m, C – H), 2,922 (m, C – H), 1,605 (m, N – O), 1,397 (s, N – O). M.P. 167.0 °C (decomp.). Elemental Analysis: calcd C 51.56% H 3.15% N 32.80%, found C 51.88% H 3.12% N 32.68%.

2-(4-aminopyrazol-1-yl)-6-(pyrazol-1-yl)pyridine (6): PtO_2•H_2O (0.0074 g, 5% catalyst loading) was suspended in a 1:1 mixture of EtOH: EtOAc (100 mL). H_2 gas was sparged through this mixture for 20 min. **5** (0.154 g, 0.599 mmol) was then added to this mixture in one portion and the stirring suspension was sparged with H_2 gas for an additional hour then sealed under a H_2 atmosphere. The sealed reaction mixture was stirred an additional 1 d at room temperature and reaction progress was monitored via TLC (5% v/v MeOH/DCM on silica). After 1 d an additional 0.007 g (5% cat. loading) PtO_2•H_2O was added to the stirring reaction accompanied by a 30 min sparge with H_2. The reaction was allowed to proceed for an additional day in a 45 °C oil bath. The reaction was then vacuum-filtered through Celite and concentrated to yield a yellow oil. This oil was subjected to silica column chromatography using a 2% v: v methanol: dichloromethane eluent. The last band (R_f = 0.10) was isolated and concentrated to give a brown crystalline solid (0.095 g, 70% yield). ^{1}H-NMR (400MHz, $CDCl_3$): 8.53 (d, 1H *J* = 2.64), 8.08 (d, 1H *J* = 0.96), 7.85 (t, 1H *J* = 8.0), 7.77-7.68 (m, 3H), 7.43 (d, 1H *J* = 1.0), 6.47 (dd, 1H *J* = 1.6, 0.7), 3.12 (s, 2H). ^{13}C{^{1}H}-NMR (100 MHz, $CDCl_3$): 150.1, 142.4, 141.2, 135.4, 131.4, 127.1, 114.0, 110.2, 108.7, 108.6, 108.0. HR-MS (ESI^+): calcd for $C_{11}H_{10}N_6$ ($[M+H]^+$) *m/z* 227.10400, found 227.10390. IR ($\bar{\nu}$, cm^{-1}): 3,347 (m, CN – H), 3,203 (m, N – H), 2,922 (m, C – H), 2852 (m, C – H) 1,602 (s, N – H), 1,578 (s, N – H). M.P. 150.2 – 158.4 °C. Elemental Analysis: calcd C 58.40% H 4.46% N 37.15%, found C 58.19% H 4.34% N 36.13%

Eu(tta)$_3$X (complexes 7 – 8): Both complexes were synthesized following the same procedure; the synthesis of complex **7** is described as a general example: Ligand **2** (0.025 g, 0.104 mmol) was combined with Eu(tta)$_3$•2H_2O (0.088 g, 0.104 mmol) and dissolved in acetone (20 mL). The solution was refluxed for 30 min, stirred at room temperature overnight and then concentrated under vacuum to give a pale brown solid. The solid was washed with hexanes, dried under vacuum and collected. We have, so far, been unable to obtain single crystals suitable for X-ray diffraction studies; bulk purity was assessed by elemental analysis and confirmed by the absence of splitting in the $5D_0 \rightarrow 7F_0$ Eu(III) ion emission spectra (indicative of one emissive species in the sample).[23]

Eu(tta)(NH$_2$)$_2$bppy (7): (83.4 mg, 76% yield) HR-MS ($MALDI^+$): calcd for $C_{27}H_{19}EuF_6N_7O_4S_2$ ($[M\text{-tta}]^+$) *m/z* 836.00509, found 836.0045. IR ($\bar{\nu}$, cm^{-1}): 3,105 (b, N – H), 2,962 (m, C – H). M.P. 104.1°C (decomp.). Elemental Analysis: calcd C 39.78% H 2.19% N 9.28%, found C 40.19% H 2.37% N 8.71%.

Eu(tta)NH$_2$bppy (8): (32.2 mg, 46% yield) HR-MS (ESI^+): calcd for $C_{35}H_{22}EuF_9N_6O_6S_3$ ($[M+Na]^+$) *m/z* 1064.97210, found 1064.97290. IR ($\bar{\nu}$, cm^{-1}): 3,131 (b, N – H), 2,926 (w, C – H). M.P. 99.2 – 145.4 °C (decomp.). Elemental Analysis: calcd C 40.35% H 2.13% N 8.07%, found C 40.59% H 2.22% N 7.01%.

Results and Discussion

Ligand Synthesis

The synthesis of the mono- and disubstituted nitro- ligands **1** and **5** was achieved via the established nucleophilic substitution of 2,6-dibromopyridine affording satisfactory yields. The synthesis of the di-substituted species **1** was achieved by reacting excess of the pyrazolate of 4-nitropyrazole and 2,6-dibromopyridine, followed by hydrogenation to yield **2**. Although it has been noted that this procedure may be expected to result in the decomposition of the 4-nitropyrazolate rather than the desired substitution,[24] we have found that by limiting the reaction temperature to 120 °C and increasing the reaction time to 7 days in diglyme yields **1** in high yield (93%). Initial attempts to form **1** using stoichiometric amounts of 4-nitropyrazole and reaction temperatures above 130 °C gave low yields and formation of the expected mono-substitution product, **3**, in yields of approximately 30%. Reaction of **3** with an additional equivalent of 4-nitropyrazole can be employed to further improve the yield of **1**. Optimization of reaction conditions such as introducing one extra equivalent of the pyrazole and NaH each, as well as extending reaction times to 7 days eventually yielded **1** in excellent yield with minimal mono-

View Article Online
DOI: 10.1039/C7DT01153A

substitution by-products. The subsequent reduction to form **2** was problematic due to the poor solubility of **1**. Limited success was achieved by reducing with $SnCl_2$ in basic media as per the literature,[25] however higher catalytic loading of Adams's catalyst and careful adjustment of the volumetric ratio of EtOH: EtOAc (2:3 was found to be optimal) enabled the desired reduction to **2** in consistent satisfactory yields in the range of 80%.

Although we did not attempt synthesis of **1** by substitution of 2,6-difluoropyridine derivatives with the pyrazolate nucleophile as has been reported previously, this may be a desirable synthetic route to pursue.[26–31] Nucleophilic aromatic substitution methods involving fluorinated pyridine starting materials may be advantageous owing to the increased reactivity of fluoride leaving groups, which may lessen the reaction time and temperature required. Additionally, employing a 4-bromo-2,6-difluoropyridine intermediate as reported by Charbonnière *et al*. may provide a path to improving the solubility of **1** via reaction of the Br- group, which would be very advantageous.[32,33]

Synthesis of the asymmetrically-substituted derivatives was also performed with similar nucleophilic substitutions followed by nitro- group reduction, but careful consideration was required when choosing the order of pyrazolate nucleophilic substitution. Attempts to synthesize **5** by treating **3** with pyrazole and NaH resulted in low yields, with large by-product formation of **4** and 4-nitropyrazole as well as bppy, indicating competition between substitution of the 4-nitropyrazole and bromine with pyrazolate. Step-wise formation of **4** via nucleophilic substitution of 2-6-dibromopyridine with pyrazole, followed by substitution with 4-nitropyrazole proved to be effective in synthesizing the mono-substituted **5**. Nucleophilic aromatic substitution using 4-aminopyrazole to directly produce **2** is undesirable, as the amine would necessitate a longer synthetic route entailing protection and deprotection steps; additionally the cost of this reactant is quite high.

Ligand Crystallography

In order to unequivocally establish the identities of **5** and **6** single crystal X-ray structures were obtained (Figure 2). In the solid state structure of **6**, a slight distortion from co-planarity with regard to the pyridine ring is apparent for the pyrazole ring bearing the primary amine, with a dihedral angle of 12.40 ° between the two heterocycles. The primary amine N–H bond distances are 0.963 Å and 0.880 Å. The difference in bond lengths arise from two distinct H-bonding interactions involving the separate H atoms, one involving an adjacent primary amine N6 (2.312 Å) and the other involving the pyrazole imine N5 atom of an adjacent 4-aminopyrazole ring (2.143 Å) (see ESI).

Ligand Spectroscopy

The results of UV-Vis absorption spectroscopy are summarized in Table 1. The absorption spectra of all ligands are characterized by two $\pi \rightarrow \pi^*$ transitions in the UV region in the range of 260 nm – 317 nm, with the exception of **2** (Figure 3.a). The bathochromic shift of the low-energy transition seen in **2** (327 nm) suggests a lower energy $n \rightarrow \pi^*$ transition combining with or completely covering the expected $\pi \rightarrow \pi^*$ transition.

Fluorescence spectroscopy of these molecules reveals excitation profiles that closely resemble the respective absorbance spectra, with excitation λ_{max} being closely associated with the λ_{max} of absorption in all cases. At room temperature, **2** and **6** exhibit broad emission peaks centered at 404 nm and 414 nm, respectively (Figure 3.b); **1** and **5** can be seen to emit very faintly in the UV region. Observation of **2**, **5** and **6** in a 2:2:1:1 volumetric ratio of ethyl iodide: diethyl ether: ethanol: toluene (EEET) solvent glass upon cooling to 77 K permitted the phosphorescence of these molecules to be observed; in the case of **2** and **6**, emission from the T_1 manifold appears as an additional shoulder in the emission spectrum of **2** centered at 486 nm and a resolved phosphorescence manifold in **6** (Figure 3.c). Identification of the blue edges of phosphorescence allowed for the determination of the T_1 energy of 25,381 cm^{-1} for **2** and 26,201 cm^{-1} for **6**. This information is of key importance in the consideration of this molecule as a sensitizing ligand for lanthanide luminescence. The blue edge of phosphorescence from **2** was determined by fitting the 77 K emission spectrum to a multi-peak Gaussian distribution model and extrapolating the resultant phosphorescence curve (see SI). In the case of **5** there appears to be significant overlap between fluorescence and phosphorescence processes, making determination of the T_1 energy level difficult; the shape and range of the 77 K emission

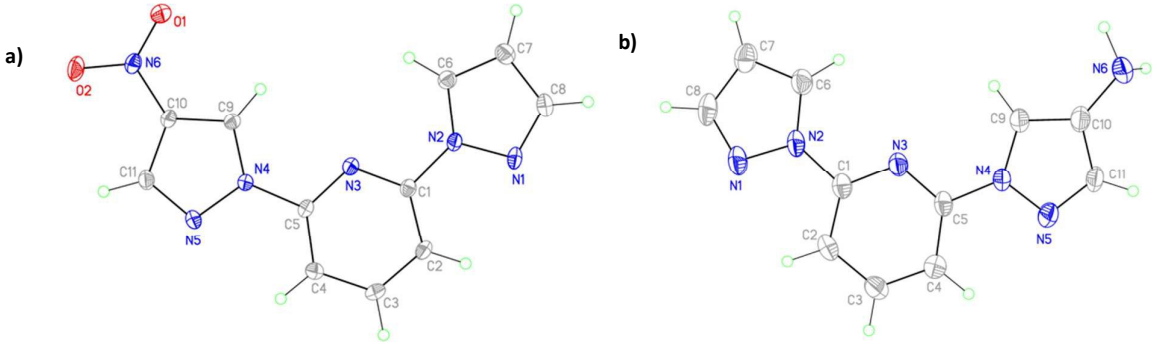

Figure 2: **a)** single crystal structure of **5**. **b)** single crystal structure of **6**. Displacement ellipsoids are scaled to the 50% probability level.

View Article Online
DOI: 10.1039/C7DT01153A

Table 1: UV-Vis absorbances of ligands and complexes in DCM solution

	1	2	5	6	7	8
λ (nm); ε ($M^{-1}cm^{-1}$)	--	--	259; 12,499	248; 18,073	266; 49,402	---
	289; 19,489	279; 5,638	276; 13,114	--	--	276; 27,902
	317; 18,397	327; 14,571	312; 14,503	314; 22,017	338; 84,565	340; 51,415

spectrum of **5** changes drastically depending on the chosen excitation wavelength, and attempts to determine emission lifetimes for phosphorescence peak identification were not possible with our current instrumentation. Excitation with the lowest-energy excitation wavelength that was discrete from the 77 K emission profile of **5** is shown in Figure 3.c, as this wavelength should maximize the phosphorescence character of the emission. This emission appears as a well-resolved manifold, though we hesitate to assign a ligand T_1 energy using the emission edge. Unfortunately no phosphorescence could be observed from **1.**

Cyclic Voltammetry

Cyclic voltammetry (CV) was performed to determine the electrochemical behavior as well as energies of the HOMO (E_{HOMO}), LUMO (E_{LUMO}), and HOMO-LUMO gap (ΔE) of these species by identifying the onset potential of each initial reductive and oxidative event of the ligands. The resultant voltammograms are shown with that of bppy under identical conditions in Figure 4; redox event peak potentials and frontier orbital energy values are reported in Table 2. Electrochemical energy levels were calculated utilizing onsets of oxidation and reduction according to equations 1 and 2.[34]

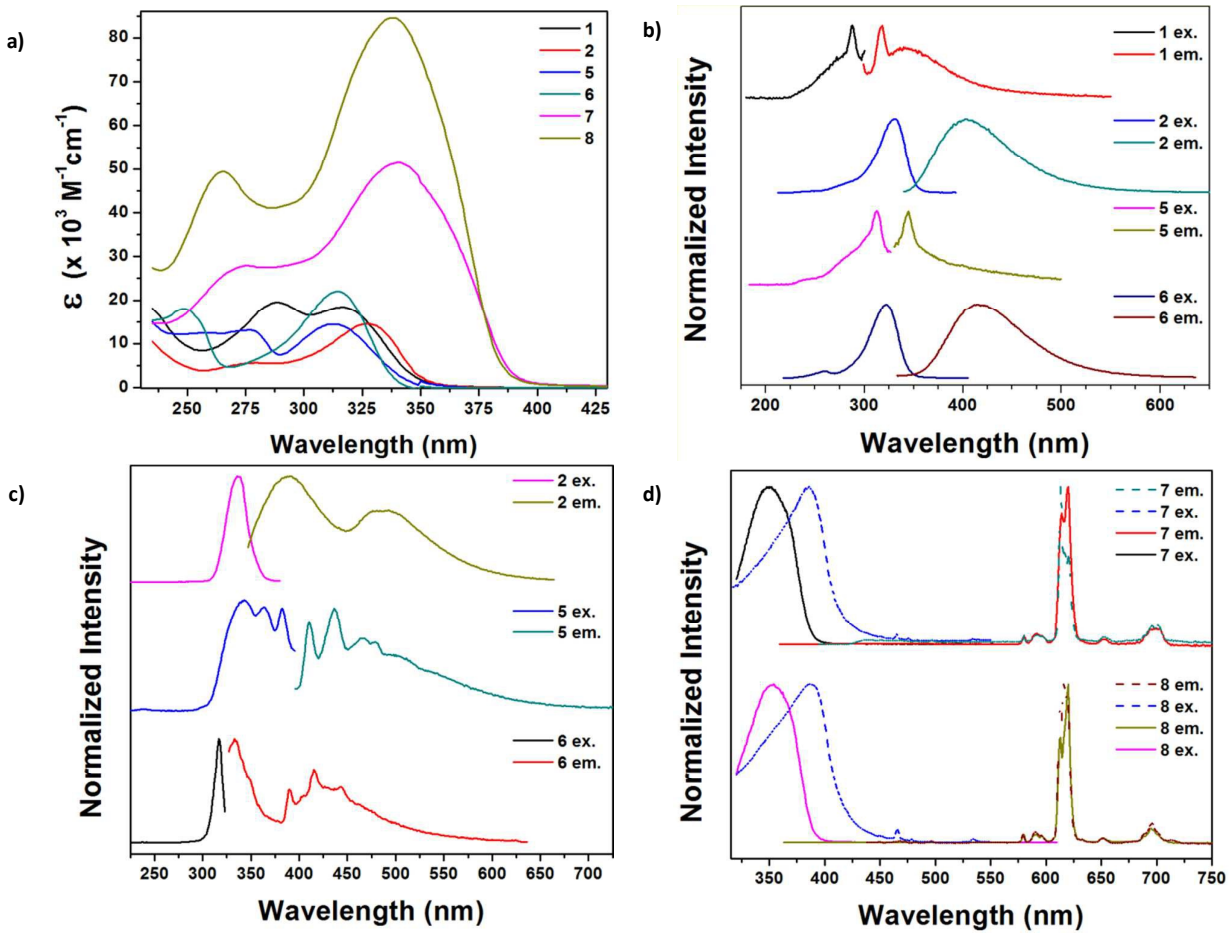

Figure 3: **a)** Absorption spectra of ligands and complexes in DCM solution **b)** Room-temperature excitation and emission spectra of ligands in DCM solution **c)** 77 K excitation and emission spectra of **2**, **5**, and **6** in solid EEET solutions **d)** DCM solution (solid lines) and solid-state (dashed lines) excitation and emission spectra of **7** and **8**.

View Article Online
DOI: 10.1039/C7DT01153A

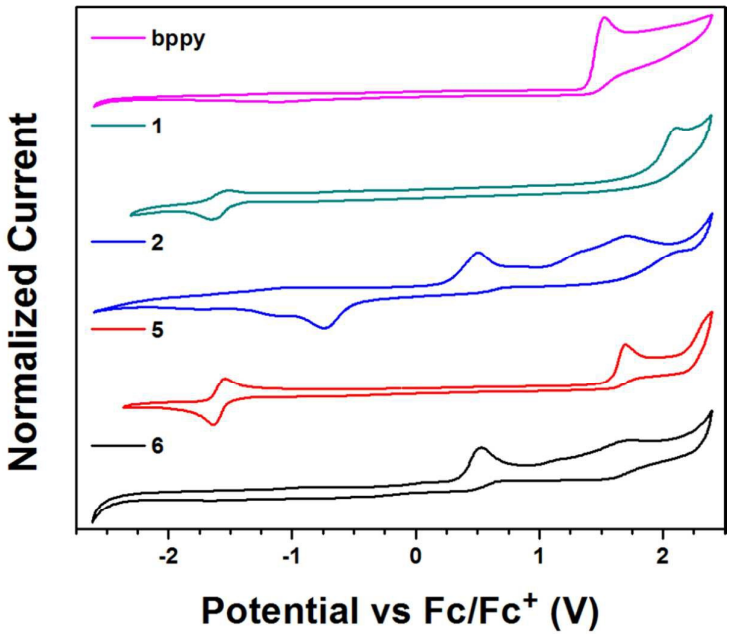

Figure 4: Cyclic voltammograms of bppy and substituted bppy derivatives in ACN solution with *t*-butylammonium hexafluorophosphate electrolyte.

$$E_{HOMO} = -\left(E_{onset,ox.vs.Fc/Fc^+} + 5.1\right)(eV) \quad (1)$$

$$E_{LUMO} = -\left(E_{onset,red.vs.Fc/Fc^+} + 5.1\right)(eV) \quad (2)$$

To the best of our knowledge, the electrochemical behavior of the parent bppy ligand has not been reported until now. Electrochemistry of bppy reveals two irreversible oxidative events at relatively high potentials; this suggests that the irreversible oxidative events seen in all of these ligands which take place at approximately 1.1 V and greater are due to the oxidation of the aromatic system, which is corroborated by the presence of similar irreversible oxidative signals in each of the rest of the series. The electron-rich or deficient nature of the amino- and nitro-bppy derivatives are reflected in the potentials at which the aromatic system is oxidized, with larger potentials being required for the molecules bearing NO_2-groups and lesser potentials required for the NH_2-bearing molecules. **1** and **5** each exhibit only one irreversible oxidative peak at positive potentials, and a reversible nitro-group redox couple upon sweeping to negative potentials. **2** and **6** undergo multiple irreversible oxidative events, and **2** can be seen to undergo two irreversible reductive events. Performing negative potential sweeps of **2** from 0 V to -2.5 V yields no reductive current, indicating coupling between the two reductive events and the oxidative events which correspond to neither bppy oxidation nor reduction of the oxidized residue; we therefore attribute these signals to redox processes undergone by the amine functionalities.

Since the reductive events evident in the voltammograms of **2** are coupled to these initial oxidative peaks and no reductive events are discernible in **6** or bppy, the E_{LUMO} of

Table 2: Cyclic voltammetry redox potentials and HOMO/LUMO energy levels of tridentate N-donors in solution

Ligand	E_{red} (V)	E_{ox} (V)	$E_{1/2}$ (V)	E_{HOMO} (eV)	E_{LUMO} (eV)	ΔE (eV)
bppy	---	1.53, 2.06	---	–6.18	–2.35	3.83
1	–1.64	–1.52, 2.11	–1.58	–7.04	–3.64	3.54
2	–1.12, –0.74	0.51, 0.86, 1.34, 1.71	---	–5.35	–1.82	3.53
5	1.64	–1.54, 1.70	–1.59	–6.68	–3.59	3.01
6	---	0.48, 1.16, 1.72	---	–5.46	–1.80	3.66

View Article Online
DOI: 10.1039/C7DT01153A

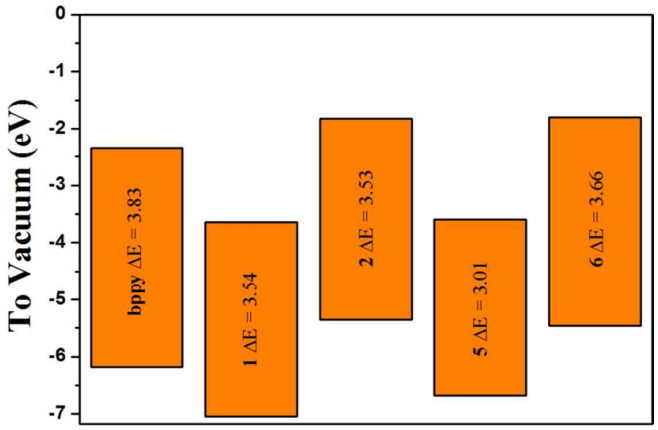

Figure 5: HOMO-LUMO gaps of the ligands described in this work.

these three ligands cannot be determined electrochemically. Therefore, the E_{LUMO} and ΔE of these molecules were calculated by combining optical measurement data with E_{HOMO} values obtained from CV studies. The energy of the red edge of the UV-Vis absorption spectra, corresponding to the 0 – 0 $S_0 \rightarrow S_1$ electronic transition, was assigned the ΔE of these ligands. The assignment of frontier orbital energies for these ligands allows for empirical LUMO energy determination and comparison across the series (Figure 5). As expected, the electron-deficient NO_2-containing ligands exhibit lowered E_{HOMO} values and raised E_{LUMO} values, whereas the electron-rich NH_2- ligands exhibit the opposite.[35–37] Interestingly, the disparity in ΔE is greatest with the mono-substituted bppy ligands whereas the di-substituted ligands exhibit nearly identical ΔE values but at different energies. In addition to serving as versatile synthetic intermediates, characterization of the electronics of these ligands indicate that they offer a means of tuning energy levels and binding strengths of bppy complexes.

Eu(III) Complex Synthesis and Spectroscopy

The new compounds were also investigated as ligands for sensitizing Eu(III) luminescence, owing to the highly-luminescent nature of the parent bppy complex.[38] Presently, all attempts at forming lanthanide complexes with **1** and **5** have failed, presumably due to the exceedingly electron-deficient nature of the ligands. However, metalation of **2** and **6** upon refluxing with $Eu(tta)_3 \bullet 2H_2O$ in acetone yielded complexes $Eu(tta)_3(NH_2)_2$bppy (**7**) and $Eu(tta)_3NH_2$bppy (**8**) (tta = 2-thenoylacetonate) (Scheme 1.c). The absorption profiles of these complexes (Figure 3.a) are primarily dominated by absorption of the tta moieties, and feature greatly enhanced absorptivity values with respect to the ligands themselves. Solution and solid-state excitation and emission spectra of these complexes are shown in Figure 3.d. The excitation spectra indicate that population of the tta chromophore excited states is responsible for sensitization of Eu(III) luminescence; the $^5D_0 \leftarrow {}^7F_0$ absorption feature of the Eu(III) ion can be seen in the excitation spectra of the solid samples. Luminescent lifetimes (τ_{obs}) and absolute quantum yields (Φ_{Eu}^{L}) were also measured. Attempts to model τ_{obs} of **7** and **8** reveals two components of luminescent relaxation in both solution and solid phases; in solution the longer-lived component appears to have a much greater contribution to the luminescence decay, whereas in the solid state, the shorter-lived decay component exhibits an increased involvement in the decay process (see Table S1). The greatly-increased contribution of the shorter lifetime in the solid state is consistent with the decreased quantum yield. By combining the weighted contributions of these components into an averaged lifetime measurement ($\tau_{obs,avg}$) (see Table S1) and calculating the radiative lifetime (τ_{rad}), it is possible to obtain an approximation of sensitization efficiency (η_{sens}) and intrinsic quantum yield (Φ_{Eu}^{Eu}) (Equations 3 – 5); these data are reported in Table 3.[39,40]

$$1/\tau_{rad} = A_{MD,0} n^3 (I_{tot}/I_{MD}) \quad (3)$$

$$\Phi_{Eu}^{Eu} = \tau_{obs}/\tau_{rad} \quad (4)$$

$$\eta_{sens} = \Phi_{Eu}^{L} / \Phi_{Eu}^{Eu} \quad (5)$$

The absence of any observable ligand luminescence in all of the luminescence emission spectra is indicative of optimal intra-complex energy matching and minimal energy loss to radiative processes (Figure 3.d). One trend that holds true for both complexes is the decrease of τ, Φ, and η_{sens} in solid-state measurements with respect to solution measurements. This may be due to stacking interactions which affect the ligand T_1 energy levels, and therefore sensitization of the Eu(III) center. Alternatively, the solid samples may allow for closer packing of the primary amine N–H oscillators and consequently greater non-radiative quenching of the chromophore excited states. We also attribute the difference in emission efficiencies of **7** and **8** to quenching involving the amine groups, as the 820 cm^{-1} difference in T_1 levels of the differing bppy ligands is unlikely to affect Eu(III) sensitization to a large extent; this is especially likely since the excitation spectra of all of these complexes are

View Article Online
DOI: 10.1039/C7DT01153A

Table 3: Photophysical characterization of Eu(III) emission of **7** and **8**

Complex	Solvent	λ_{ex} (nm)	τ_{obs} (μs)	$\tau_{obs,avg}$ (μs)	Φ_{Eu}^{L} (%)	τ_{rad} (μs)	Φ_{Eu}^{Eu} (%)	η_{sens} (%)
7	DCM	350	66 ± 9; 380 ± 10	339	24.2 ± 0.8	1,150	29	82
	solid	386	60 ± 2; 212 ± 2	132	1.1 ± 0.2	615	21	5
8	DCM	353	160 ± 20; 490 ± 10	424	30 ± 2	821	52	58
	solid	386	41 ± 3; 361 ± 6	252	10.2 ± 0.1	726	35	29

suggestive of Eu(III) luminescence occurring at wavelengths corresponding with light absorption of the tta moieties. Current research is underway to improve the luminescent efficiency of the amino-bppy complexes by synthetic modifications to remove the amine N–H oscillators in an effort to minimize excited-state quenching.[41]

Conclusions

We report four new nitro- or amino-substituted derivatives of bppy, their electronic properties, and have successfully demonstrated the utility of two of these ligands in sensitizing lanthanide luminescence.

The synthesis and characterization of the bppy derivatives described in this work should allow for further expansion of the library of possible ligands with an even larger range of electronic and chemical environments. Future studies will be focused on 4-pyrazolyl- hydroxylamines,[42,43] secondary or tertiary amines, amides, imines, nitroamines, azoxy compounds,[44] and diazonium salts.[45] Additionally, **2** and **6** lend themselves well to the formation of products resulting from a wealth of diazonium substitution chemistry, such as *bis*- aryl-, azido-,[46] azo-,[47] cyano-, fluoro-, hydroxyl-,[48] and mercapto- substituted bppy species, as well as those made possible by Buchwald-Hartwig amination conditions. The formation of **3** also presents the opportunity for asymmetric syntheses of bppy derivatives containing different substituents at either 4-position of the pyrazole rings, as is common in nucleophilic aryl substitution synthetic routes. Additionally, with established synthetic routes to form both mono- and di-substituted terminal amino-bppy ligands (**2** and **6**), condensation polymerization of bppy for Wolf Type II metallopolymer syntheses, and numerous other supramolecular structures that avoid the use of expensive metal catalysts are now possible.[38–41]

Efforts in our group involving these new ligands are currently directed toward the synthesis of novel bppy architectures which exploit the reactivity of these primary aryl amines and nitro-compounds for targeted applications in the area of emissive materials.

Acknowledgements

The authors would like to gratefully acknowledge the Welch Foundation (F-1631 and F-816) for providing financial support.

References

1 M. A. Halcrow, *Coord. Chem. Rev.*, 2009, **253**, 2493–2514.
2 L. D. Carlos, R. A. S. Ferreira, V. de Z. Bermudez and S. J. L. Ribeiro, *Adv. Mater.*, 2009, **21**, 509–534.
3 X. Wang, H. Chang, J. Xie, B. Zhao, B. Liu, S. Xu, W. Pei, N. Ren, L. Huang and W. Huang, *Coord. Chem. Rev.*, 2014, **273–274**, 201–212.
4 V. Fernández-Moreira, B. Song, V. Sivagnanam, A.-S. Chauvin, C. D. B. Vandevyver, M. Gijs, I. Hemmilä, H.-A. Lehr and J.-C. G. Bünzli, *Analyst*, 2009, **135**, 42–52.
5 D. L. Jameson, J. K. Blaho, K. T. Kruger and K. A. Goldsby, *Inorg. Chem.*, 1989, **28**, 4312–4314.
6 M. A. Halcrow, *New J. Chem.*, 2014, **38**, 1868–1882.
7 G. Zoppellaro and M. Baumgarten, *Eur. J. Org. Chem.*, 2005, **2005**, 2888–2892.
8 X. J. Zhu and B. J. Holliday, *Macromol. Rapid Commun.*, 2010, **31**, 904–909.
9 S. Basak, P. Hui and R. Chandrasekar, *Synthesis*, 2009, **2009**, 4042–4048.
10 S. Basak, Y. S. L. V. Narayana, M. Baumgarten, K. Müllen and R. Chandrasekar, *Macromolecules*, 2013, **46**, 362–369.
11 Y. S. L. V. Narayana, D. Venkatakrishnarao, A. Biswas, M. A. Mohiddon, N. Viswanathan and R. Chandrasekar, *ACS Appl. Mater. Interfaces*, 2016, **8**, 952–958.
12 Y. S. L. V. Narayana, S. Basak, M. Baumgarten, K. Müllen and R. Chandrasekar, *Adv. Funct. Mater.*, 2013, **23**, 5875–5880.
13 Y. S. L. V. Narayana, M. Baumgarten, K. Müllen and R. Chandrasekar, *Macromolecules*, 2015, **48**, 4801–4812.
14 S. Basak, P. Hui, S. Boodida and R. Chandrasekar, *J. Org. Chem.*, 2012, **77**, 3620–3626.
15 R. Pritchard, C. A. Kilner, S. A. Barrett and M. A. Halcrow, *Inorganica Chim. Acta*, 2009, **362**, 4365–4371.
16 Y. Fukuda, A. Nakao and K. Hayashi, *J. Chem. Soc. Dalton Trans.*, 2002, 527–533.
17 K. S. Kumar, B. Schäfer, S. Lebedkin, L. Karmazin, M. M. Kappes and M. Ruben, *Dalton Trans.*, 2015, **44**, 15611–15619.
18 M. Pietraszkiewicz, O. Pietraszkiewicz, J. Karpiuk, A. Majka, G. Dutkiewicz, T. Borowiak, A. M. Kaczmarek and R. Van Deun, *J. Lumin.*, 2016, **170**, **Part 2**, 411–419.
19 A. Zaïm, H. Nozary, L. Guénée, C. Besnard, J.-F. Lemonnier, S. Petoud and C. Piguet, *Chem. – Eur. J.*, 2012, **18**, 7155–7168.
20 P. A. Smith, C. Crawford, N. Beedoe, Z. Assefa and R. E. Sykora, *Inorg. Chem.*, 2012, **51**, 12230–12241.
21 H. Gallardo, G. Conte, A. J. Bortoluzzi, I. H. Bechtold, A. Pereira, W. G. Quirino, C. Legnani and M. Cremona, *Inorganica Chim. Acta*, 2011, **365**, 152–158.

View Article Online
DOI: 10.1039/C7DT01153A

22 C. R. De Silva, J. R. Maeyer, R. Wang, G. S. Nichol and Z. Zheng, *Inorganica Chim. Acta*, 2007, **360**, 3543–3552.
23 W. D. Horrocks and M. Albin, in *Progress in Inorganic Chemistry*, ed. S. J. Lippard, John Wiley & Sons, Inc., Hoboken, NJ, USA, 1984, vol. 31, pp. 1–104.
24 R. Mohammed, G. Chastanet, F. Tuna, T. L. Malkin, S. A. Barrett, C. A. Kilner, J.-F. Létard and M. A. Halcrow, *Eur. J. Inorg. Chem.*, 2013, **2013**, 819–831.
25 E. V. Govor, A. B. Lysenko, D. Quiñonero, E. B. Rusanov, A. N. Chernega, J. Moellmer, R. Staudt, H. Krautscheid, A. Frontera and K. V. Domasevitch, *Chem. Commun.*, 2011, **47**, 1764–1766.
26 M. Schlosser and T. Rausis, *Helv. Chim. Acta*, 2005, **88**, 1240–1249.
27 L. Wang, N. Liu and B. Dai, *RSC Adv.*, 2015, **5**, 82097–82111.
28 L. J. Kershaw Cook, R. Kulmaczewski, R. Mohammed, S. Dudley, S. A. Barrett, M. A. Little, R. J. Deeth and M. A. Halcrow, *Angew. Chem. Int. Ed.*, 2016, **55**, 4327–4331.
29 A. Santoro, L. J. Kershaw Cook, R. Kulmaczewski, S. A. Barrett, O. Cespedes and M. A. Halcrow, *Inorg. Chem.*, 2015, **54**, 682–693.
30 L. Pukenas, F. Benn, E. Lovell, A. Santoro, L. J. K. Cook, M. A. Halcrow and S. D. Evans, *J. Mater. Chem. C*, 2015, **3**, 7890–7896.
31 M. Starck, L. Charbonnière and R. Ziessel, *Synthesis*, 2013, **45**, 837–844.
32 P. Kadjane, M. Starck, F. Camerel, D. Hill, N. Hildebrandt, R. Ziessel and L. J. Charbonnière, *Inorg. Chem.*, 2009, **48**, 4601–4603.
33 M. Starck, P. Kadjane, E. Bois, B. Darbouret, A. Incamps, R. Ziessel and L. J. Charbonnière, *Chem. – Eur. J.*, 2011, **17**, 9164–9179.
34 C. M. Cardona, W. Li, A. E. Kaifer, D. Stockdale and G. C. Bazan, *Adv. Mater.*, 2011, **23**, 2367–2371.
35 Y. Huang, M. Zhang, L. Ye, X. Guo, C. C. Han, Y. Li and J. Hou, *J. Mater. Chem.*, 2012, **22**, 5700–5705.
36 K. Krumova and G. Cosa, *J. Am. Chem. Soc.*, 2010, **132**, 17560–17569.
37 M. Al-Anber, B. Milde, W. Alhalasah, H. Lang and R. Holze, *Electrochimica Acta*, 2008, **53**, 6038–6047.
38 J. M. Wilkerson, The University of Texas at Austin, 2012.
39 K. Binnemans, *Coord. Chem. Rev.*, 2015, **295**, 1–45.
40 M. H. V. Werts, R. T. F. Jukes and J. W. Verhoeven, *Phys. Chem. Chem. Phys.*, 2002, **4**, 1542–1548.
41 J.-C. G. Bünzli, *Coord. Chem. Rev.*, 2015, **293–294**, 19–47.
42 A. Tallec, R. Hazard, J. SuwiNski and P. Wagner, *Pol. J. Chem.*, 2000, **47**, 1177–1183.
43 P. Cuadrado, A. M. González-Nogal and S. Martínez, *Tetrahedron*, 1997, **53**, 8585–8598.
44 J. Suwiński and P. Wagner, *Pol. J. Chem.*, 2000, **74**, 1575–1580.
45 P. Yin, J. Zhang, D. A. Parrish and J. M. Shreeve, *Chem. - Eur. J.*, 2014, **20**, 16529–16536.
46 J. M. Fevig, J. Cacciola, J. Buriak Jr., K. A. Rossi, R. M. Knabb, J. M. Luettgen, P. C. Wong, S. A. Bai, R. R. Wexler and P. Y. S. Lam, *Bioorg. Med. Chem. Lett.*, 2006, **16**, 3755–3760.
47 R. Kumar, Y. C. Joshi and P. Joshi, *Heterocycl. Commun.*, 2005, **11**, 361–364.
48 F. De Sio, *Heterocycles*, 1984, **22**, 2309–2311.

View Article Online
DOI: 10.1039/C7DT01153A

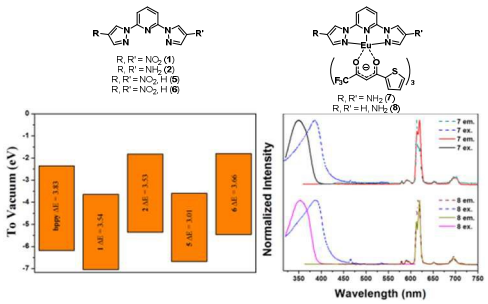

The synthesis of nitro- and amino-*bis*(pyrazol-1-yl)pyridines was achieved, allowing for tuning of frontier orbital energies and Eu(III) complex spectroscopic investigations.